



# Investigation of beam window buckling with consideration of irradiation effects for conceptual ADS design

Takanori Sugawara\*, Kenji Kikuchi, Kenji Nishihara, Hiroyuki Oigawa

Japan Atomic Energy Agency, Shirakata Shirane 2-4, Tokai-mura, Naka-gun, Ibaraki, 319-1195, Japan

## ABSTRACT

The investigation of the beam window, which is a key component in the conceptual design of an Accelerator Driven System, has been performed. In the past studies, it was found that buckling failure due to hydrostatic pressure in the liquid lead bismuth was critical failure mode for the beam window and detailed structural analyses were performed. These investigations, however, did not consider irradiation effects by neutrons and protons. In this study, investigations based on the latest knowledge for irradiation effects obtained in the spallation target irradiation program are presented. By using the experimental data, it was found that the buckling pressure increased about 80% by the irradiation (20 dpa). It was assumed that if the beam window had integrity in the unirradiated condition, the buckling failure would not be critical issue during the ADS operation.

© 2009 Elsevier B.V. All rights reserved.

## 1. Introduction

To reduce the burden for the geological disposal of the high level waste (HLW), an Accelerator Driven System (ADS) has been studied to transmute minor actinides (MA) included in the HLW. The ADS investigated in Japan Atomic Energy Agency (JAEA) is a lead bismuth eutectic (LBE) cooled subcritical system [1]. A high intensity proton accelerator with 1.5 GeV beam energy and a subcritical core with 800 MW thermal power is designed to transmute 250 kg MA per year in the system. Fig. 1 shows a conceptual structure of the ADS.

Since the ADS is a hybrid system of an accelerator and a nuclear reactor, there are many technical issues to be solved for the accelerator, LBE as a coolant and a target and the subcritical core. The structural integrity of the beam window, which is the boundary between the accelerator and the subcritical core, is one of the most important issues in the ADS, and therefore needs R&D. In the past studies [2], it was found that the buckling failure due to hydrostatic pressure in the liquid lead bismuth was critical failure mode for the beam window from the simplified assessment using “design by analysis” approach for a nuclear power plant. Detailed structural analyses were explored to find a solution for avoiding instantaneous buckling. The results showed that the ellipse shape concepts were acceptable under the current ADS design parameters [2].

However, these investigations did not consider irradiation effects by neutrons and protons. The irradiation causes many

changes for the beam window such as irradiation hardening, embrittlement, swelling and DBTT shift for martensitic steel material. It is indispensable to consider irradiation effects for the investigations of the beam window. This study treats the effect of the irradiation hardening to the beam window integrity based on the latest knowledge obtained in the spallation target irradiation program (STIP) [3] at the Swiss Spallation Neutron Source (SINQ).

The following sections present a selection of the experimental data to introduce irradiation effects to the buckling analysis and detailed conditions for the buckling analysis. Throughout this study, T91 (Mod. 9Cr–1Mo) steel is employed as the material for a beam window model.

## 2. Selection of experimental data

### 2.1. Required data for buckling analysis

The buckling analysis has been carried out by using a finite element method (FEM) calculation code, FINAS [4] developed by CRC Corporation and JAEA. In the FINAS calculation, material data as follows are required; (1) Young's modulus ( $E$ ), (2) Poisson's ratio ( $\nu$ ), (3) thermal expansion coefficient ( $\alpha$ ), (4) yield stress (YS) and (5) work hardening coefficient ( $H'$ ). In this study, it was assumed that the changes of  $E$ ,  $\nu$  and  $\alpha$  would be very small by neutrons and protons irradiation, so the T91 data [5] employed in the past studies were used for these three parameters. The data prepared in Ref. [5] are the revised data investigated in Ref. [6] for the R&D of the fast reactor.

It was considered that the change of YS and  $H'$  would be significant by the irradiation. However, detailed investigations for the

\* Corresponding author. Tel.: +81 29 282 6436; fax: +81 29 282 5671.  
E-mail address: [sugawara.takanori@jaea.go.jp](mailto:sugawara.takanori@jaea.go.jp) (T. Sugawara).

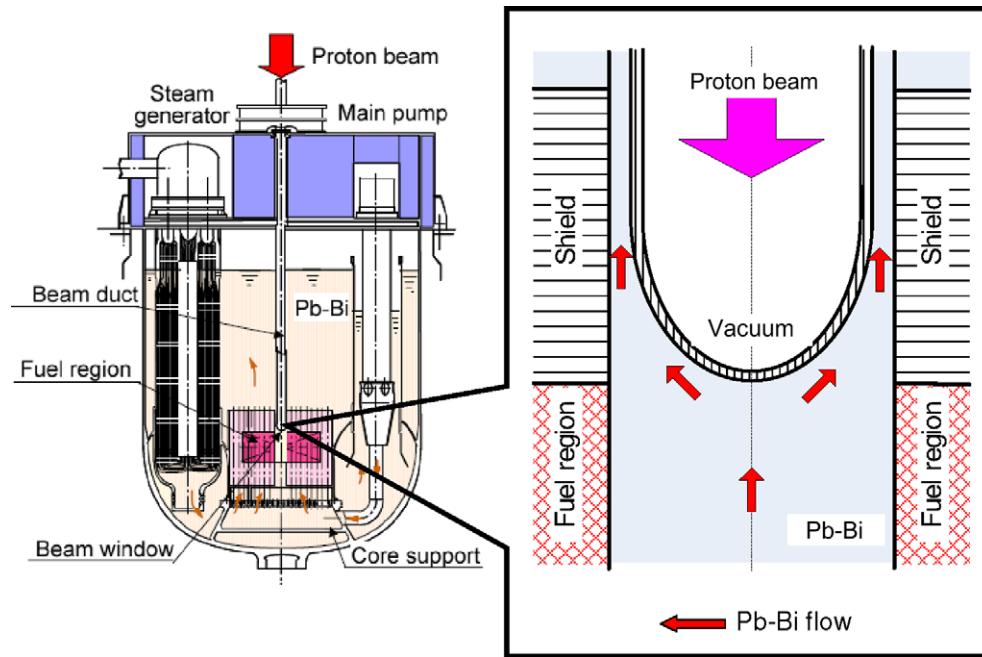


Fig. 1. Conceptual structure of LBE cooled ADS (beam window is the boundary between Pb-Bi region and vacuum region).

change of  $H'$  were not performed and provisional data of  $H'$  were prepared in this study. This is because the change of  $H'$  has little meaning in the buckling analysis since  $H'$  represents the rate of change of stress with strain in the plastic region. On the other hand, the change of YS affects the structural strength. Therefore, selection of experimental data for YS was performed based on the experimental data.

## 2.2. Selection of experimental data

Fig. 2 shows relations between displacement dose and YS for STIP-III experiment. In this figure,  $T_{\text{test}}$  means the temperature at which the tensile test was performed. The displacement dose was up to 20 dpa by the 580 MeV proton beam (SINQ) and the irradiation temperature was up to 560 °C. In this experiment, T91 samples normalized at 1040 °C for 1 h, rapidly cooled, and then

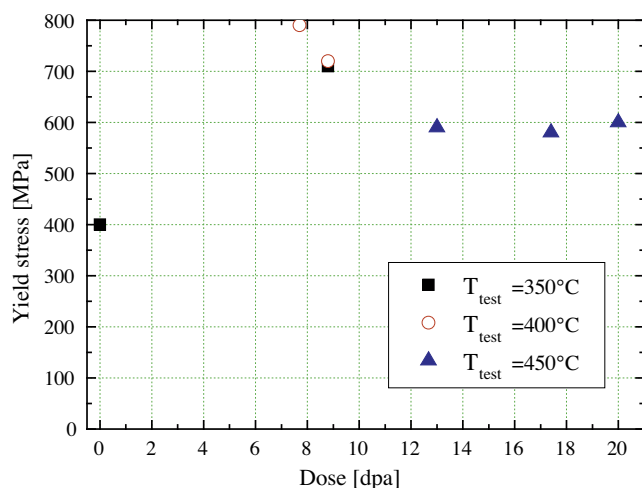


Fig. 2. Relation between displacement dose and YS for T91 steel in STIP-III experiment [3].

tempered at 760 °C for 1 h were employed. Tensile tests at 25, 350, 400 and 450 °C were carried out although the tensile results at room temperature are not shown in this figure. Since the range of the temperature of the beam window investigated in JAEA was about 400–500 °C in normal operation, the data of STIP III as shown ' $T_{\text{test}} = 450^\circ\text{C}$ ' in Fig. 2 were employed as the experimental data.

Table 1 compares parameters between the STIP-III experiment and JAEA's ADS. The dose and production for  $^4\text{He}$  for the ADS are calculation results in Ref. [7]. It was found that the proton beam energy and the temperature condition are widely different. The envisaged dose of the ADS is much larger than that of STIP III. However, for the production of  $^4\text{He}$ , the amount of STIP III at the maximum temperature was larger than that of the ADS.

It was assumed that these differences were caused by the difference of proton/neutron contribution. In the ADS analysis, the doses caused by the protons and the neutrons were 4.5 and 50.6 dpa, respectively [7]. Additionally, for the neutron contribution, the doses caused by high energy neutrons (above 10 MeV) and low energy neutrons from the subcritical core (below 10 MeV) were 3.6 and 47.0 dpa, respectively. This means that the contribution of neutrons from the subcritical core was about 85% in the ADS condition. On the other hand, there was no contribution of neutrons from a subcritical core in STIP III. It was considered that the contribution of protons in STIP III was much larger than that of neutrons although these comparisons were not described in Ref. [3]. Therefore, the production for  $^4\text{He}$  in STIP III was larger than that in the

Table 1  
Comparison of parameters between STIP-III experiment [3] and ADS [7].

	STIP III	ADS
Proton energy (GeV)	0.58	1.5
Temperature (°C)	180–560 <sup>a</sup>	400–500 <sup>b</sup>
Dose (dpa)	7.7–20.2	55 [/ $300\text{EFPD}$ ] <sup>c</sup>
$^4\text{He}$ production (appm)	520–1710	825 [/ $300\text{EFPD}$ ] <sup>c</sup>

<sup>a</sup> Average irradiation temperature.

<sup>b</sup> Beam window temperature during operation.

<sup>c</sup> Integrated value for 300 effective full power days.

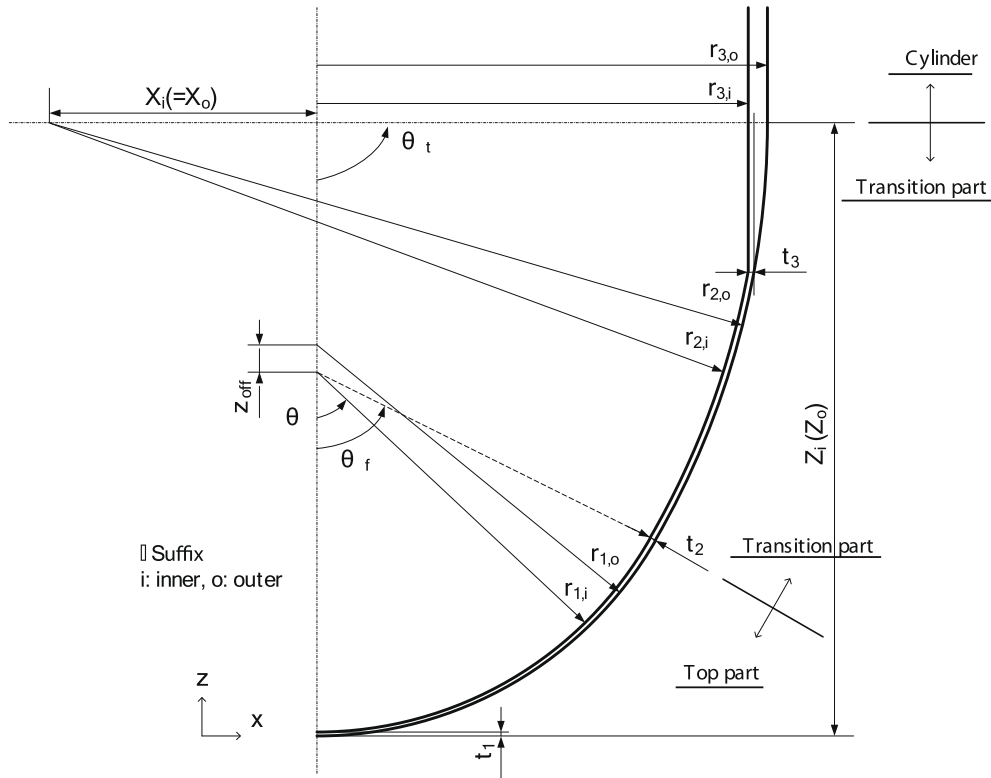


Fig. 3. Generalized calculation model.

ADS though the dose in STIP III was much smaller than that in the ADS.

3. Calculation conditions

3.1. Calculation model

The previous studies [2] showed that an ellipse concept was suitable to prevent the buckling failure in the condition of ADS design concept. In Ref. [8], a parametric survey to create the feasible ellipse concept was performed. The generalized calculation model shown in Fig. 3 was employed in the parametric survey and it was indicated that some concepts were acceptable under the current ADS design parameters. The generalized calculation model was also employed in this analysis with a two-dimensional calculation model, which consisted of the quadrangle element.

Table 2  
Parameters of calculation model (unit except  $\theta_f$  is (mm)).

Parameters	Values
$t_1$	2.0
$t_2$	3.0
$t_3$	3.0
$r_{1,i}$	200.0
$r_{2,i}$	490.9
$r_{3,i}$	225.0
$r_{1,o}$	204.0
$r_{2,o}$	493.9
$r_{3,o}$	235.0
$\theta_f$ (degree)	60.0
$X_i (=X_o)$	-258.9
$Z_i$	334.9
$Z_o$	335.0
$Z_{off}$	1.985

The generalized calculation model is an ellipse model which consists of a top part, a transition part and a cylinder part. Inner or outer surfaces of the top and transition parts are expressed as mathematical formulas and are connected at  $\theta_f = 60^\circ$  smoothly. In the previous investigation [8],  $t_1$ ,  $t_2$  and  $t_3$  which were the thicknesses at the top,  $\theta_f = 60^\circ$ , and a connection between the transition and cylinder parts were treated as parameters. In this study,  $t_1/t_2/t_3 = 2.0/3.0/3.0$  mm which was the typical suitable concept in the previous investigation was employed. The main other parameters are presented in Table 2.

3.2. Temperature condition

The buckling failure occurs by both the primary stress (e.g., external pressure) and the secondary stress (e.g., thermal stress).

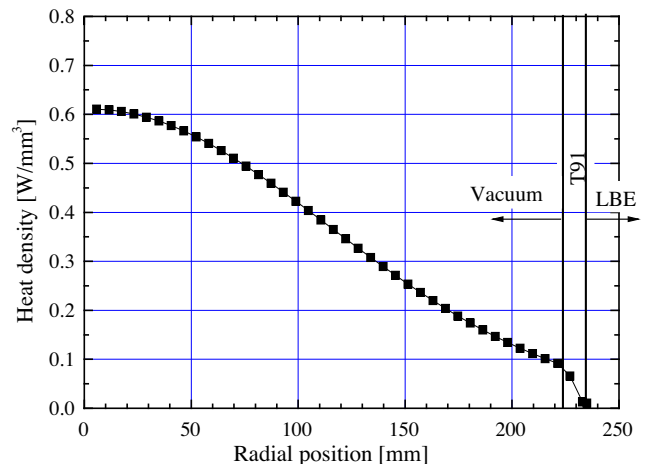


Fig. 4. Heat density distribution.

Detailed temperature distributions were calculated and employed in the structure analyses since it was found that the main cause of the buckling failure was the thermal stress due to the proton beam in the previous studies [2,8].

The temperature distribution was calculated as a function of thickness, heat density and coolant temperature. The temperature  $T_M$  at the depth  $t_M$  ( $0 \leq t_M \leq t_0, t_0$  is the thickness) was calculated by following equations:

$$T_0 = T_F(\theta) + Q_0(r) \cdot t_0/\alpha \tag{1}$$

$$T_M = T_0 + Q_0(r) \cdot \left(\frac{t_0^2}{2}\right) \left\{ 1 - \left(\frac{t_M}{t_0}\right)^2 \right\} / \lambda \tag{2}$$

where  $T_0$  is the temperature at the outer surface of the beam window,  $T_F(\theta)$  is the temperature of the coolant,  $Q_0(r)$  is the heat density,  $\alpha$  is the heat transfer coefficient between the coolant and the

beam window ( $=3.95 \text{ W/cm}^2/\text{°C}$ ) and  $\lambda$  is the thermal conductivity for the beam window ( $=0.27 \text{ W/cm/°C}$ ).

The heat transfer coefficient  $\alpha$  was the average value calculated by the computational fluid dynamics (CFD) analysis, which was performed by STAR-CD [9] in Ref. [10]. The coolant temperature distribution  $T_F(\theta)$  calculated by STAR-CD in Ref. [10] were also used in this survey.

The heat density distribution  $Q_0(r)$  was calculated by the cross-section data for heat generation [7] and flux distributions of protons and neutrons. The flux distribution of protons and neutrons above 20 MeV was calculated by PHITS code [11] which is a general-purpose particles and heavy ion transport Monte Carlo code, and that of neutrons below 20 MeV was calculated by TWODANT code [12] which is a deterministic neutron transport calculation code. Fig. 4 shows the heat density distribution for the case of 1.5 GeV–20 mA proton beam. Temperature distributions calculated by this heat density distribution are presented in Fig. 5.

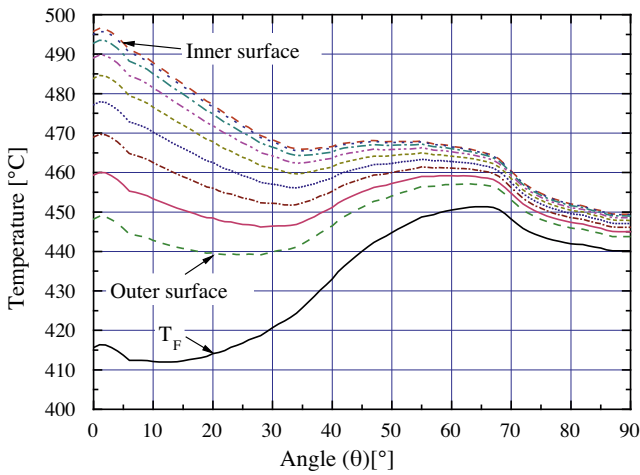


Fig. 5. Temperature distribution in the beam window.

### 3.3. Calculation case

Two calculation cases were carried out. The first case is one without the irradiation effect. In this case, the YS data prepared in Ref. [5] were employed. The second case is one with the irradiation effect. In this case, the material data for ‘ $T_{\text{test}} = 450 \text{ °C}$ ’ shown in Fig. 2 were adapted uniformly to all elements in the calculation model. In this case, Young’s modulus  $E$ , Poisson’s ratio  $\nu$  and thermal expansion coefficient  $\alpha$  were given as the function of temperature based on Ref. [5] and the YS data were given as the constant (600 MPa).

## 4. Results and discussions

### 4.1. Buckling pressure

The buckling pressures were 10.6 and 18.8 MPa in the cases without and with the irradiation effect, respectively. From these calculation results, it was confirmed that the buckling pressure in-

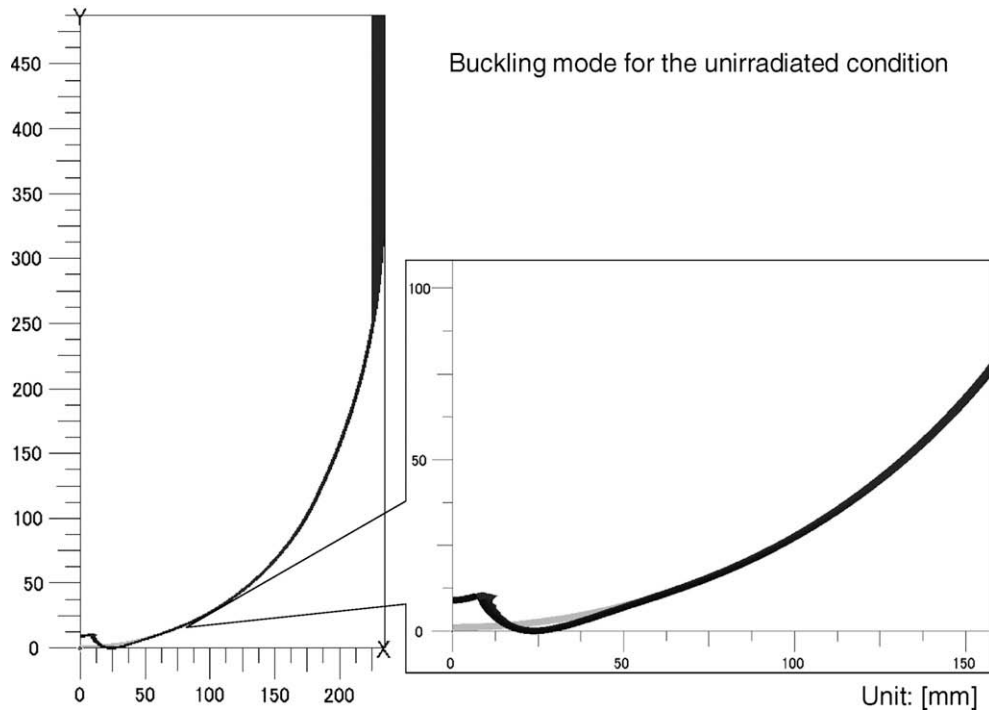


Fig. 6. Buckling mode for the unirradiated condition by eigen mode calculation.

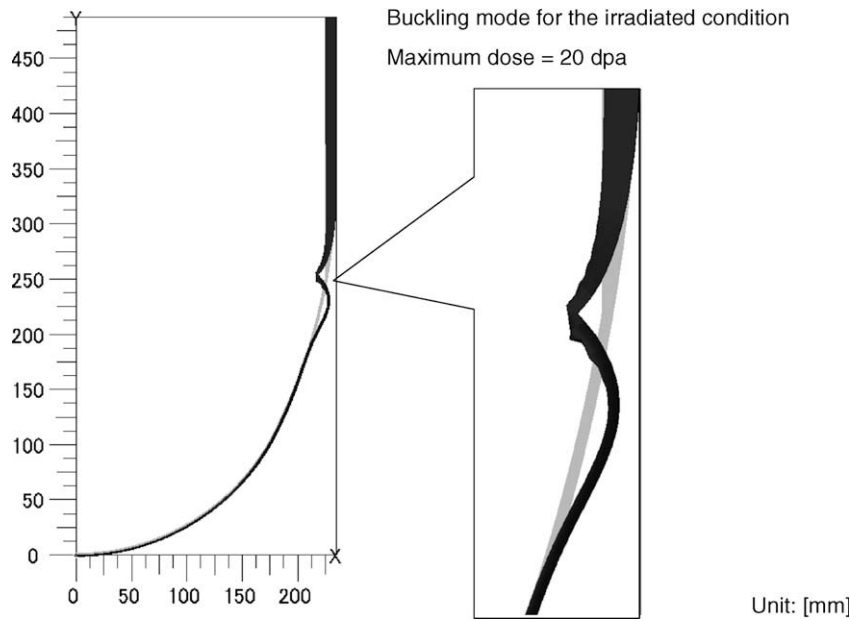


Fig. 7. Buckling mode for the irradiated condition by eigen mode calculation.

creased by the irradiation in the current design condition. The buckling pressure with 20 dpa was about 1.8 times larger than that with the unirradiated condition. It was supposed that the buckling pressure would increase moreover if the temperature of the beam window decreased.

#### 4.2. Buckling mode

Eigen mode calculation was also performed to know the buckling mode for each case. Fig. 6 shows the buckling mode for the unirradiated condition. In this condition, the buckling failure would occur at the top of the beam window. This failure mode was expected from the previous studies [8] since the load at a top position was significant due to the heat generation by protons.

Fig. 7 illustrates the buckling mode for the case with the irradiation effect. In this calculation, the material data for 20 dpa were adopted to all elements. In this case, the tendency of the buckling mode was different from the previous calculation case. The buckling mode did not appear at the top of the beam window and it was found at a connection position between the window and the cylinder part. Since the strength of the top part increased by the irradiation, that of the connection position decreased, relatively.

The buckling failure has been one of the most serious failure modes for the beam window in the unirradiated condition. However, if the beam window has integrity in the unirradiated condition, the buckling failure will not be the serious problem during the ADS operation due to the increase of  $Y_S$  by the irradiation. It is necessary to investigate embrittlement, swelling and DBTT shift for martensitic steel as the next step for the beam window investigation.

#### 5. Conclusions

The investigation of the beam window which is the critical issue for the ADS has been performed. Since the previous investigations [2,8] did not consider irradiation effects by neutrons and protons,

this study treats the effect of irradiation hardening to the beam window based on the latest knowledge obtained in STIP.

Through the selection of the experimental data and the buckling analysis by FEM, it was found that the buckling pressure increased by the irradiation. In the case with the irradiation effect, the buckling pressure increased about 80% when the maximum dose was 20 dpa. It was also confirmed that the buckling mode changed by the irradiation. The buckling was observed at the top of the beam window in the unirradiated condition. However, the buckling appeared at the connection position between the window and the cylinder part in the case with the irradiation effect. It is concluded that if the beam window had integrity in the unirradiated condition, then the buckling failure would not be the serious problem during the ADS operation.

#### References

- [1] K. Tsujimoto, T. Sasa, K. Nishihara, H. Oigawa, H. Takano, J. Nucl. Sci. Technol. 41 (1) (2004) 21.
- [2] T. Sugawara, K. Suzuki, K. Nishihara, T. Sasa, Y. Kurata, K. Kikuchi, H. Oigawa, JAEA-Research 2008-026, 2008.
- [3] Z. Tong, Y. Dai, IWSMT9, October, 2008.
- [4] CRC Solutions Corporation and Japan Atomic Energy Agency, Finas, Finite Element Nonlinear Structural Analysis System, Commercial Code, 2006.
- [5] FBR Materials Evaluation (FME) Subcommittee of Japan Welding Engineering Society, Material Technology of FBR Development, Japan Welding Engineering Society, 1999.
- [6] Power Reactor and Nuclear Fuel Development Corporation, PNC TN9410 88-105, 1988.
- [7] K. Nishihara, K. Kikuchi, J. Nucl. Mater. 377 (2008) 298.
- [8] T. Sugawara, K. Suzuki, K. Nishihara, T. Sasa, Y. Kurata, K. Kikuchi, H. Oigawa, in: Proceedings of the 10th Information Exchange Meeting on Actinide and Fission Product Partitioning and Transmutation, OECD/NEA, 6–10 October 2008, Mito, Japan, in press.
- [9] Computational Dynamics Ltd., "STAR-CD," CFD Commercial Code, London, England.
- [10] S. Saito, K. Tsujimoto, K. Kikuchi, Y. Kurata, T. Sasa, M. Umeno, K. Nishihara, M. Mizumoto, N. Ouchi, H. Takei, H. Oigawa, Nucl. Instrum. Methods Phys. Res. A 562 (2006) 646.
- [11] H. Iwase, K. Niita, T. Nakamura, J. Nucl. Sci. Technol. 39 (11) (2002) 1142.
- [12] Users Guide for TWODANT: A Code Package for Two-Dimensional, Diffusion-Accelerated, Neutral-Particle Transport, LA-10049-M, 1990.